

Reconfigurable Coding Design for Programmable Metasurface-Based DOA Estimation via Riemannian Manifold Optimization

Changcheng Hu^{ID}, Ruoyu Zhang^{ID}, Member, IEEE, Guangyi Chen^{ID}, Xuewen Luo^{ID}, Member, IEEE,
Xinrong Guan^{ID}, and Chau Yuen^{ID}, Fellow, IEEE

Abstract—Programmable metasurface (PMS) has effective control over amplitude and phase, presenting a cost-efficient solution for direction-of-arrival (DOA) estimation. However, its performance is significantly influenced by the design of the PMS's reconfigurable coding. In this letter, we propose a reconfigurable coding design method for PMS-based DOA estimation problem based on Riemannian manifold optimization. Specifically, we cast the reconfigurable coding design as a mutual coherence minimization problem, and reformulate it as a Frobenius norm minimization problem, aiming to reduce the difference between the identity matrix and the Gram matrix of the sensing matrix. To address this non-convex optimization problem, we propose an alternating optimization framework that combines positive semidefinite programming with Riemannian manifold optimization to obtain the reconfigurable coding matrix. Simulation results validate that the proposed method outperforms the existing methods in DOA estimation accuracy with fewer measurements.

Index Terms—Programmable metasurface, direction-of-arrival estimation, mutual coherence, reconfigurable coding design, Riemannian manifold optimization.

I. INTRODUCTION

AS A critical technology in array signal processing, direction-of-arrival (DOA) estimation plays a significant role in various applications such as radar, wireless communications, and positioning systems [1], [2], [3]. However, to achieve higher estimation accuracy, it is often necessary

Received 21 May 2025; revised 17 July 2025; accepted 3 August 2025. Date of publication 12 August 2025; date of current version 8 January 2026. This work was supported in part by the National Natural Science Foundation of China under Grant 62571248, Grant 62201266, and Grant 62171461; in part by the Key Laboratory of Intelligent Space TTC&O (Space Engineering University), Ministry of Education under Grant CYK2025-01-12; in part by the China Postdoctoral Science Foundation under Grant 2025M773483; in part by the Postdoctoral Fellowship Program of China Postdoctoral Science Foundation under Grant GZC20252297; and in part by the Ministry of Education, Singapore, under its MOE Tier 2 under Award T2EP50124-0032. The associate editor coordinating the review of this article and approving it for publication was J.-C. Chen. (*Corresponding author: Ruoyu Zhang*)

Changcheng Hu, Ruoyu Zhang, and Guangyi Chen are with the Key Laboratory of Near Range RF Sensing ICs & Microsystems (NJUST), Ministry of Education, School of Electronic and Optical Engineering, Nanjing University of Science and Technology, Nanjing 210094, China (e-mail: huchangcheng@njust.edu.cn; ryzhang19@njust.edu.cn; gyi@njust.edu.cn).

Xuewen Luo is with the School of Computer Science and Engineering, Northeastern University, Shenyang 110169, China (e-mail: luoxw@cse.neu.edu.cn).

Xinrong Guan is with the College of Communications Engineering, Army Engineering University of PLA, Nanjing 210007, China (e-mail: guanxr@aliyun.com).

Chau Yuen is with the School of Electrical and Electronics Engineering, Nanyang Technological University, Singapore 639798 (e-mail: chau.yuen@ntu.edu.sg).

Digital Object Identifier 10.1109/LWC.2025.3598026

to increase the aperture of the antenna array in multiple-input multiple-output (MIMO) systems, which may incur prohibitive complications such as complex hardware architectures, increased circuit complexity, and higher implementation costs [4], [5].

In recent years, programmable metasurface (PMS) has emerged as a promising solution due to its superior control over both amplitude and phase [6], [7], [8], [9], [10]. Cui et al. [11] introduced the concept of digital coding metasurfaces, describing these surfaces in terms of binary codes. To obtain the source direction, the authors in [12] proposed a novel DOA estimation method based on amplifier-integrated active metasurface, where the typical multiple signal classification was employed. To further improve the performance of DOA estimation, the authors in [13] applied a compressive sensing (CS)-based method to PMS-aided DOA estimation system models. In [14], the authors proposed a PMS-based Ka-band DOA estimation mechanism, where the orthogonal matching pursuit (OMP) algorithm is used to estimate the DOA from a sparsely sampled dataset. The authors in [15] proposed a novel DOA estimation method based on the atomic norm, considering the position perturbations of the uncrewed aerial vehicle (UAV), where the atomic norm is defined by the position disturbance parameters. To overcome the high computational complexity of high-accuracy DOA algorithms on UAVs with limited processing power, the authors of [16] proposed a hybrid optoelectronic neural network that estimates DOA using only amplitude observations.

Although the aforementioned CS-based algorithms offer promising DOA estimation accuracy and efficiency, their performance is limited by the reconfigurable coding matrix, which determines the mutual coherence of the sensing matrix in the CS framework [17]. The authors in [18] designed training vectors such that the total coherence of the equivalent sensing matrix is minimized. In [19], the authors proposed to optimize the precoding matrix to approach the sum rate performance of the fully digital MIMO systems based on manifold optimization (MO). However, the aforementioned sensing matrix optimization methods are all developed for conventional MIMO systems and it is necessary to propose an effective reconfigurable coding design for PMS-based DOA systems with one-bit controllable phases.

In this letter, we propose a reconfigurable coding design method for PMS-based DOA estimation based on Riemannian MO. We first establish a PMS-based single-channel system model and formulate the coding design as a mutual coherence minimization problem of the sensing matrix. The problem is relaxed into a Frobenius norm optimization framework

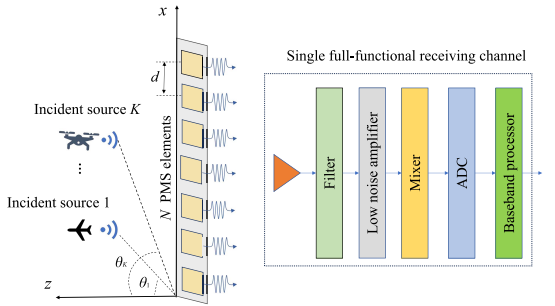


Fig. 1. Programmable metasurface-based DOA estimation system model.

to approximate the Gram matrix to an identity matrix. To address the non-convexity, we propose an alternating optimization (AO) strategy combining semidefinite programming with Riemannian MO algorithms. Simulations show that the proposed method outperforms the existing methods in DOA estimation accuracy and resolution probability while requiring fewer measurements.

Notations: The identity matrix of dimension N is represented as \mathbf{I}_N . Additionally, $\|\cdot\|$ represents the norm, $\text{diag}(\cdot)$ and $\text{blkdiag}(\cdot)$ represent diagonal and block diagonal matrices, respectively. The operators \circ , \otimes , $\text{vec}(\cdot)$ and $\text{invec}(\cdot)$ denote Hadamard product, Kronecker product, vectorization and inverse vectorization operations, respectively. $\mathbf{A}(i,j)$ is the i th row and j th column of matrix \mathbf{A} , and $\text{Re}\{\cdot\}$ denotes the real part of a complex number.

II. SYSTEM MODEL

As shown in Fig. 1, we assume that there are K incident sources, and the PMS consists of N elements, with equal spacing d between adjacent PMS elements. The transmitted signal from the n th PMS element at the m th measurement is given by

$$x_{n,m} = \sum_{k=1}^K s_k e^{j \frac{2\pi}{\lambda} (n-1)d \sin \theta_k} + v_{n,m}, \quad (1)$$

where λ represents the wavelength, s_k is the incident signal from the k th target source, $p_s = |s_k|^2$, $k = 1, 2, \dots, K$, θ_k denotes the incident angle of the k th target source and $v_{n,m} \sim \mathcal{CN}(0, p_v)$ represents additive white Gaussian noise.

The signal passing through the transmissive PMS at the m th measurement undergoes changes in phases, expressed as

$$\tilde{x}_{n,m} = e^{j \phi_{n,m}} x_{n,m}, \quad (2)$$

where $\phi_{n,m}$ in \mathcal{W} represents the transmission phase of the n th PMS element in the m th measurement, and $\mathcal{W} = \{e^{j \frac{2\pi b}{2^B}} \mid b = 1, 2, \dots, 2^B\}$ denotes the B -bit quantized phase set. At the receiver, we only use a single receiving channel, which includes filters, a low-noise amplifier, a mixer, an analog-to-digital converter, and a baseband processor, all of which process the received signals. Let d_n be the distance between the n th PMS element and the receiving channel, the received signal of the single receiving channel at the m th measurement can be expressed as

$$y_m = \sum_{n=1}^N \tilde{x}_{n,m} e^{j \frac{2\pi}{\lambda} d_n} + \tilde{v}_m = \mathbf{p}_m^T \mathbf{W}(\boldsymbol{\theta}) \mathbf{s} + \mathbf{v}_m + \tilde{v}_m, \quad (3)$$

where $\boldsymbol{\theta} = [\theta_1, \theta_2, \dots, \theta_K]^T \in \mathbb{C}^{K \times 1}$, $\mathbf{s} = [s_1, s_2, \dots, s_K]^T \in \mathbb{C}^{K \times 1}$, $\mathbf{v}_m = [v_{1,m}, v_{2,m}, \dots, v_{N,m}]^T \in \mathbb{C}^{N \times 1}$ denotes the noise in the array signal received by the PMS during the m th measurement, and $\tilde{v}_m \sim \mathcal{CN}(0, p_{\tilde{v}})$ is the thermal noise from the PMS. The matrix $\mathbf{W} = \text{diag}(\mathbf{w}) \in \mathbb{C}^{N \times N}$ represents the phase change of the signal from the PMS to the receiving channel with the diagonal vector being $\mathbf{w} = [e^{j \frac{2\pi}{\lambda} d_1}, e^{j \frac{2\pi}{\lambda} d_2}, \dots, e^{j \frac{2\pi}{\lambda} d_N}]^T \in \mathbb{C}^{N \times 1}$. We define the steering matrix as

$$\mathbf{A}(\boldsymbol{\theta}) = [\mathbf{a}(\theta_1), \mathbf{a}(\theta_2), \dots, \mathbf{a}(\theta_K)] \in \mathbb{C}^{N \times K}, \quad (4)$$

where $\mathbf{a}(\theta_k)$ denotes the steering vector, which is expressed as $\mathbf{a}(\theta_k) = [1, e^{j \frac{2\pi}{\lambda} d \sin \theta_k}, \dots, e^{j \frac{2\pi}{\lambda} (N-1) d \sin \theta_k}]^T \in \mathbb{C}^{N \times 1}$. In (3), we define a vector \mathbf{p}_m that represents the amplitude-phase parameters of PMS at the m th measurement as

$$\mathbf{p}_m = [e^{j \phi_{1,m}}, e^{j \phi_{2,m}}, \dots, e^{j \phi_{N,m}}]^T \in \mathbb{C}^{N \times 1}. \quad (5)$$

Then, by collecting all M measurements, the received signal $\mathbf{y} = [y_1, y_2, \dots, y_M]^T \in \mathbb{C}^{M \times 1}$ can be concatenated as

$$\mathbf{y} = \mathbf{P} \mathbf{W} \mathbf{A}(\boldsymbol{\theta}) \mathbf{s} + \tilde{\mathbf{W}} \mathbf{v} + \tilde{\mathbf{v}}, \quad (6)$$

where $\tilde{\mathbf{v}} = [\tilde{v}_1, \tilde{v}_2, \dots, \tilde{v}_M]^T \in \mathbb{C}^{M \times 1}$, and $\mathbf{P} = [\mathbf{p}_1, \mathbf{p}_2, \dots, \mathbf{p}_M]^T \in \mathbb{C}^{M \times N}$ is the reconfigurable coding matrix that represents the amplitude-phase parameters of PMS. In addition, $\mathbf{v} = [\mathbf{v}_1^T, \mathbf{v}_2^T, \dots, \mathbf{v}_M^T]^T \in \mathbb{C}^{MN \times 1}$, $\tilde{\mathbf{W}} = \text{blkdiag}(\mathbf{p}_1^T, \mathbf{p}_2^T, \dots, \mathbf{p}_M^T) \in \mathbb{C}^{M \times MN}$, and $\tilde{\mathbf{W}} = \mathbf{I}_M \otimes \mathbf{W} \in \mathbb{C}^{MN \times MN}$.

III. PROPOSED RECONFIGURABLE CODING DESIGN

In this section, we propose a reconfigurable coding design method, which includes an AO framework that combines positive semidefinite programming with Riemannian MO to obtain the reconfigurable coding matrix.

A. Formulation for Reconfigurable Coding Design

Different from conventional methods that only configure phase shifts of PMS elements, we introduce a surrogate matrix $\mathbf{F} \in \mathbb{C}^{M \times M}$ with constraint $\|\mathbf{F}(:, m)\|^2 = 1$, $m = 1, \dots, M$. Accordingly, the received signal can be expressed as

$$\bar{\mathbf{y}} = \mathbf{F} \mathbf{P} \mathbf{W} \mathbf{A}(\boldsymbol{\theta}) \mathbf{s} + \mathbf{F} \tilde{\mathbf{W}} \mathbf{v} + \mathbf{F} \tilde{\mathbf{v}} = \mathbf{F} \mathbf{P} \mathbf{W} \bar{\mathbf{s}} + \bar{\mathbf{v}}, \quad (7)$$

where the second equality holds by dividing the entire space into G regions ($G \gg K$), $\bar{\mathbf{s}} = [\mathbf{a}(\varphi_1), \dots, \mathbf{a}(\varphi_G)] \in \mathbb{C}^{N \times G}$, $\bar{\mathbf{s}} = [s_1, s_2, \dots, s_G]^T \in \mathbb{C}^{G \times 1}$ has K non-zero elements, and $\bar{\mathbf{v}} = \mathbf{F} \mathbf{P} \mathbf{W} \mathbf{v} + \mathbf{F} \tilde{\mathbf{v}} \in \mathbb{C}^{M \times 1}$ is the total noise vector. In addition, when \mathbf{F} is the identity matrix, the expression reduces to the classical signal model given in (6). Now, the DOA estimation problem in (7) is transformed to a sparse signal recovery problem in the framework of compressed sensing, where the indices of non-zero elements in $\bar{\mathbf{s}}$ is corresponding to the DOA.

For the performance evaluation of sparse recovery algorithms, an important metric is the mutual coherence of the sensing matrix $\bar{\mathbf{Q}} = \mathbf{F} \mathbf{P} \mathbf{W} \bar{\mathbf{A}} \in \mathbb{C}^{M \times G}$, which is expressed as [20]

$$\mu(\bar{\mathbf{Q}}) = \max_{g \neq g'} \frac{|\mathbf{q}_g^H \mathbf{q}_{g'}|}{\|\mathbf{q}_g\| \|\mathbf{q}_{g'}\|}, \quad (8)$$

where \mathbf{q}_g and $\mathbf{q}_{g'}$ are two different columns of $\bar{\mathbf{Q}}$. The μ in (8) is challenging to optimize directly, so we relax the problem by minimizing the Frobenius norm of the difference between the identity matrix and the Gram matrix of $\bar{\mathbf{Q}}$ [18], which can be written as

$$\begin{aligned} \min_{\mathbf{F}, \mathbf{P}} & \|\bar{\mathbf{A}}^H \mathbf{W}^H \mathbf{P}^H \mathbf{F}^H \mathbf{F} \mathbf{P} \mathbf{W} \bar{\mathbf{A}} - \mathbf{I}_G\|_F^2 \\ \text{s.t. } & \mathbf{P}(m, n) \in \mathcal{W}, \|\mathbf{F}(:, m)\|^2 = 1. \end{aligned} \quad (9)$$

In the following, we propose an AO algorithm for reconfigurable coding design that consists of two phases: the design of \mathbf{F} and the design of \mathbf{P} .

B. The Design of \mathbf{F}

We first consider the design of \mathbf{F} while keeping \mathbf{P} fixed, which can be expressed as

$$\begin{aligned} \min_{\mathbf{F}} & \|\bar{\mathbf{A}}^H \mathbf{W}^H \mathbf{P}^H \mathbf{F}^H \mathbf{F} \mathbf{P} \mathbf{W} \bar{\mathbf{A}} - \mathbf{I}_G\|_F^2 \\ \text{s.t. } & \|\mathbf{F}(:, m)\|^2 = 1. \end{aligned} \quad (10)$$

For (10), we introduce an intermediate variable $\mathbf{X} = \mathbf{F}^H \mathbf{F} \in \mathbb{C}^{M \times M}$, which is a positive semi-definite matrix. Thus, (10) can be rewritten as

$$\begin{aligned} \min_{\mathbf{F}} & \|\bar{\mathbf{A}}^H \mathbf{W}^H \mathbf{P}^H \mathbf{X} \mathbf{P} \mathbf{W} \bar{\mathbf{A}} - \mathbf{I}_G\|_F^2 \\ \text{s.t. } & \mathbf{X} \succeq 0, \mathbf{X}(m, m) = 1, \end{aligned} \quad (11)$$

which has already been transformed into a convex expression, hence we can solve it using various methods, such as the generic CVX solver. Let $\hat{\mathbf{X}}$ be the solution of (11), then \mathbf{F} can be obtained as [20]

$$\mathbf{F} = \hat{\Sigma}_{\hat{\mathbf{X}}}^{\frac{1}{2}} \hat{\mathbf{V}}_{\hat{\mathbf{X}}}^H, \quad (12)$$

where $\hat{\Sigma}_{\hat{\mathbf{X}}}$ and $\hat{\mathbf{V}}_{\hat{\mathbf{X}}}$ represent the matrices composed of the M eigenvalues and eigenvectors of $\hat{\mathbf{X}}$, respectively.

C. The Design of \mathbf{P}

In this subsection, we will design \mathbf{P} by fixing \mathbf{F} . We first consider the case where \mathbf{P} has infinite resolution. By quantizing the phase of the aforementioned continuous-phase solution, we can obtain an approximately optimal solution with discrete phases. When the resolution is infinite, the problem can be expressed as

$$\begin{aligned} \min_{\mathbf{P}} & \|\bar{\mathbf{A}}^H \mathbf{W}^H \mathbf{P}^H \mathbf{F}^H \mathbf{F} \mathbf{P} \mathbf{W} \bar{\mathbf{A}} - \mathbf{I}_G\|_F^2 \\ \text{s.t. } & |\mathbf{P}(m, n)| = 1. \end{aligned} \quad (13)$$

The non-convexity presents challenges in finding the optimal solution. However, although the constraints in (13) are non-convex, they are smooth. Therefore, we can treat the constraints in (13) as a specific manifold [19], and then transform it into an unconstrained optimization problem on the complex circle manifold by exploiting the MO theory.

Motivated by [20], we can vectorize \mathbf{P} to obtain a constant vector $\mathbf{x} = \text{vec}(\mathbf{P}) \in \mathbb{C}^{MN \times 1}$, which forms a complex circle manifold, i.e.,

$$\mathcal{M} = \{\mathbf{x}: |\mathbf{x}| = 1_{MN,1}\}, \quad (14)$$

where the manifold \mathcal{M} is a topological structure where each point is endowed with a local Euclidean structure. Specifically, each point on the manifold has a neighborhood that is homeomorphic to Euclidean space. For a given point \mathbf{x} on the manifold \mathcal{M} , its tangent space $T_x \mathcal{M}$ is defined as the set of all tangent vectors ξ_x , where each ξ_x is tangent to any curve passing through the point \mathbf{x} on \mathcal{M} .

Based on (13) and (14), the cost function is equivalently given by

$$f(\mathbf{x}) = \|\bar{\mathbf{A}}^H \mathbf{W}^H \text{invec}(\mathbf{x})^H \mathbf{F}^H \mathbf{F} \text{invec}(\mathbf{x}) \mathbf{W} \bar{\mathbf{A}} - \mathbf{I}_G\|_F^2, \quad (15)$$

where $\text{invec}(\mathbf{x})$ corresponds to the matrix \mathbf{P} . Additionally, its Euclidean gradient is given by

$$\nabla f(\mathbf{x}) = 4 \text{vec} \left(\mathbf{F}^H \mathbf{F} \text{invec}(\mathbf{x}) \mathbf{W} \bar{\mathbf{A}} \left(\bar{\mathbf{A}}^H \mathbf{W}^H \text{invec}(\mathbf{x})^H \right. \right. \\ \left. \left. \mathbf{F}^H \mathbf{F} \text{invec}(\mathbf{x}) \mathbf{W} \bar{\mathbf{A}} - \mathbf{I}_G \right) \bar{\mathbf{A}}^H \mathbf{W}^H \right). \quad (16)$$

To minimize the deviation of the update of \mathbf{x} from the manifold, we obtain the Riemannian gradient by orthogonally projecting the Euclidean gradient $\nabla f(\mathbf{x})$ onto the tangent space $T_x \mathcal{M}$ [19], which can be written as

$$\text{grad} f(\mathbf{x}) = \nabla f(\mathbf{x}) - \text{Re}\{\nabla f(\mathbf{x}) \circ \mathbf{x}^*\} \circ \mathbf{x}. \quad (17)$$

Given a point $\mathbf{x}_k \in \mathcal{M}$ and a search direction $\mathbf{d}_k \in T_{\mathbf{x}_k} \mathcal{M}$, a line search can be performed to move along \mathbf{d}_k to the point $\mathbf{x}_k + \alpha_k \mathbf{d}_k \in T_{\mathbf{x}_k} \mathcal{M}$, where α_k is the step size. However, the resulting vector $\mathbf{x}_k + \alpha_k \mathbf{d}_k$ no longer lies on the manifold \mathcal{M} [21]. To achieve this, a **retraction** mapping operator [22] $\mathcal{R}_{\mathbf{x}_k}: T_{\mathbf{x}_k} \mathcal{M} \rightarrow \mathcal{M}$ is employed to project the point $\mathbf{x}_k + \alpha_k \mathbf{d}_k$ back onto the manifold \mathcal{M} , ensuring the next iteration remains on \mathcal{M} , which can be expressed as

$$\mathbf{x}_{k+1} = \mathcal{R}_{\mathbf{x}_k}(\alpha_k \mathbf{d}_k) = \frac{\mathbf{x}_k + \alpha_k \mathbf{d}_k}{\|\mathbf{x}_k + \alpha_k \mathbf{d}_k\|}. \quad (18)$$

Furthermore, since $\text{grad} f(\mathbf{x}_{k+1})$ and \mathbf{d}_k belong to different points on the manifold \mathcal{M} , the conjugate gradient method in Euclidean space cannot be directly applied to the conjugate gradient method on the manifold \mathcal{M} . To implement the conjugate gradient algorithm on \mathcal{M} , we need a mechanism to transport tangent elements from one tangent space $T_{\mathbf{x}_k} \mathcal{M}$ to another $T_{\mathbf{x}_{k+1}} \mathcal{M}$. This operation is performed by the vector **transport** $\mathcal{T}_{\mathbf{x}_k \rightarrow \mathbf{x}_{k+1}}: T_{\mathbf{x}_k} \mathcal{M} \rightarrow T_{\mathbf{x}_{k+1}} \mathcal{M}$, which can be expressed as [22]

$$\mathcal{T}_{\mathbf{x}_k \rightarrow \mathbf{x}_{k+1}}(\mathbf{d}_k) = \mathbf{d}_k - \text{Re}\{\mathbf{d}_k \circ \mathbf{x}_{k+1}^*\} \circ \mathbf{x}_{k+1}. \quad (19)$$

Then, the search direction $\mathbf{d}_{k+1} \in T_{\mathbf{x}_{k+1}} \mathcal{M}$ for the conjugate gradient method can be computed as

$$\mathbf{d}_{k+1} = -\text{grad} f(\mathbf{x}_{k+1}) + \beta_{k+1} \mathcal{T}_{\mathbf{x}_k \rightarrow \mathbf{x}_{k+1}}(\mathbf{d}_k), \quad (20)$$

where β_{k+1} is a weight parameter for keeping the objective function non-increasing in each iteration, which can be calculated using Polak-Ribiere formula [22].

Based on the MO method, we derive a continuous-phase reconfigurable coding matrix. This matrix is further discretized into the final discrete-phase reconfigurable coding matrix \mathbf{P} through a quantization function $\mathcal{Q}(\cdot)$, which maps a complex unit-norm variable to its nearest point in the set \mathcal{W} .

To summarize, the detailed steps of the proposed reconfigurable coding design algorithm are outlined in **Algorithm 1**. The proposed algorithm initializes a random-phase matrix \mathbf{P}_0 and iteratively optimizes the hybrid structure by first solving subproblems (11) and (12) to update \mathbf{F} while fixing \mathbf{P} ,

Algorithm 1 Proposed Reconfigurable Coding Design Based on Riemannian MO

Input: $\mathbf{W}, \bar{\mathbf{A}}$.

- 1: **Initialization:** Construct \mathbf{P}_0 with random phases, $k = 0$;
- 2: **repeat**
- 3: Optimize \mathbf{F}_{k+1} with fixed \mathbf{P}_k by solving (11) and (12);
- 4: Get \mathbf{P}_{k+1} with fixed \mathbf{F}_{k+1} by MO method;
- 5: $k = k + 1$;
- 6: **until** a stopping criterion triggers.
- 7: Obtain $\mathbf{F}_{\text{opt}} = \mathbf{F}_k$, and $\mathbf{P}_{\text{opt}} = \mathcal{Q}(\mathbf{P}_k)$;
- 8: The optimized equivalent sensing matrix $\bar{\mathbf{Q}}_{\text{opt}} = \mathbf{F}_{\text{opt}} \mathbf{P}_{\text{opt}} \mathbf{W} \bar{\mathbf{A}}$;

Output: $\bar{\mathbf{Q}}_{\text{opt}}$.

followed by updating \mathbf{P} via MO with fixed \mathbf{F} . This alternating process continues until a stopping criterion is met, yielding the optimized hybrid matrices \mathbf{F}_{opt} and \mathbf{P}_{opt} , and the resulting equivalent sensing matrix $\bar{\mathbf{Q}}_{\text{opt}}$ as the final output.

The time and space complexity of the proposed method are analyzed as follows. The time complexity of Step 3 in Algorithm 1 is $\mathcal{O}(M^3)$, and the time complexity of Step 4 is $\mathcal{O}(MN^2)$. The matrix multiplication in Step 8 requires $\mathcal{O}(M^2N + MN^2 + MNG)$. The overall time complexity is $\mathcal{O}(I(M^3 + MN^2) + M^2N + MNG)$, where I is the number of iterations. The space complexity is analyzed as follows. Solving \mathbf{F}_{opt} requires $\mathcal{O}(M^2)$ space, while solving \mathbf{P}_{opt} requires $\mathcal{O}(MN)$ space. Additionally, the matrix multiplication operations require $\mathcal{O}(MG)$ extra space. Therefore, the overall space complexity is $\mathcal{O}(M^2 + MN + MG)$.

IV. SIMULATION RESULTS AND ANALYSIS

In this section, we conduct the numerical simulations, where we set $d = \lambda/2$, $N = 32$, $G = 120$, $B = 1$, $p_{\tilde{v}} = 0$ and signal-to-noise ratio (SNR) is defined as p_s/p_v . The number of alternating optimization iterations is set to $I = 5$. The grids φ_g are determined so that $\sin(\varphi_g)$ are uniformly distributed in $[-1, 1]$, i.e., $\sin(\varphi_g) = \frac{2}{G}(g - 1) - 1$, $g = 1, \dots, G$. To investigate the performance of the proposed reconfigurable coding design, the following baselines are considered: Baseline 1: The method using a random coding matrix [13]. Baseline 2: The method that optimizes only \mathbf{P} via MO [23], without employing AO. Baseline 3: The method in [20], which does not include the diagonal element constraint specified in (11).

The root mean square error (RMSE) is defined as $\sqrt{\frac{1}{JK} \sum_{j=1}^J \sum_{k=1}^K (\hat{\theta}_{jk} - \theta_k)^2}$, where J represents the number of Monte Carlo trials, and we set $J = 1000$. $\hat{\theta}_{jk}$ denotes the estimated value of the k th angle in the j th Monte Carlo trial, and θ_k represents the true angle of the k th target.

To evaluate the resolution performance of the proposed algorithm, a typical metric called resolution probability is introduced, which is defined as $|\hat{\theta}_p - \theta_p| < |\theta_1 - \theta_2|/2$, where $\hat{\theta}_p, p = 1, 2$ denotes the estimated angle of the target.

Fig. 2 presents the histogram of the off-diagonal elements of the normalized Gram matrix for both optimized and

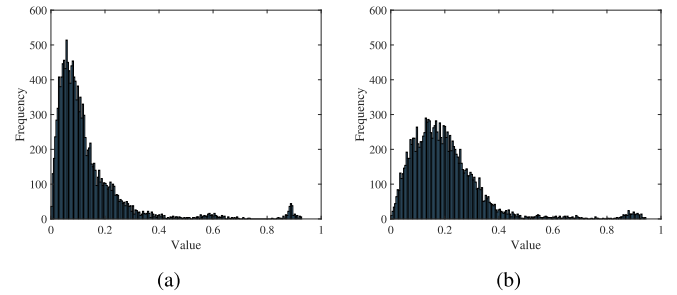


Fig. 2. Histogram of the off-diagonal elements of the normalized Gram matrix for (a) the proposed method and (b) Baseline 1.

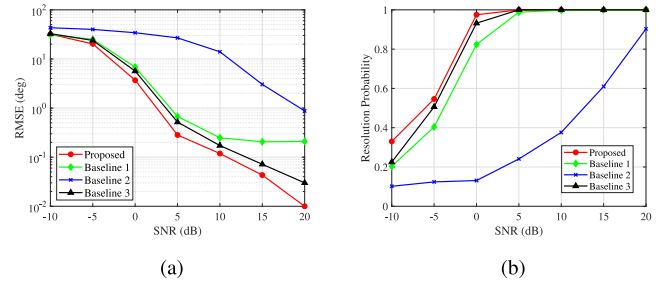


Fig. 3. (a) RMSE and (b) resolution probability of DOA estimation using the proposed methods and baselines versus SNR for two target angles, 9.97° and 42.72° .

random sensing matrices with $M = 24$. The (i, j) th element of the normalized Gram matrix of $\bar{\mathbf{Q}}$ is calculated by $|\mathbf{q}_i^H \mathbf{q}_j| / (\|\mathbf{q}_i\| \|\mathbf{q}_j\|)$, where \mathbf{q}_i and \mathbf{q}_j are two different columns of $\bar{\mathbf{Q}}$. For the random matrix, the off-diagonal elements are predominantly distributed between 0 and 0.4, with a peak near 0.2. In contrast, the optimized matrix exhibits a concentration of off-diagonal elements below 0.2, peaking around 0.1. This shows that the proposed optimization effectively reduces these values, lowering mutual coherence and improving the sensing matrix's orthogonality.

Fig. 3 compares the RMSE and resolution probability of DOA estimation at $M = 20$ for the proposed method and baselines. Under the same SNR, the proposed method achieves lower DOA estimation errors and higher resolution probabilities compared to all the baselines, indicating that the proposed method reduces the SNR requirements. The figure also shows that DOA estimation performance is poor when only \mathbf{P} is optimized without AO, highlighting the importance of AO.

Fig. 4 evaluates the DOA estimation resolution probability by varying two target angles, both ranging from -60° to 60° , represented along the x - and y -axes, while the z -axis indicates the resolution probability under each angle pair. The results show that the proposed method consistently achieves high resolution probability when the angular separation exceeds a certain threshold, outperforming all other methods. Although Baseline 3 shows improvements over the random sensing matrix, its performance still lags behind the proposed approach. Additionally, Fig. 4(c) demonstrates that optimizing only the parameter \mathbf{P} without adopting the AO framework leads to significantly lower resolution probability.

Fig. 5 compares the resolution probability of DOA estimation using the proposed method and the baselines, as a function

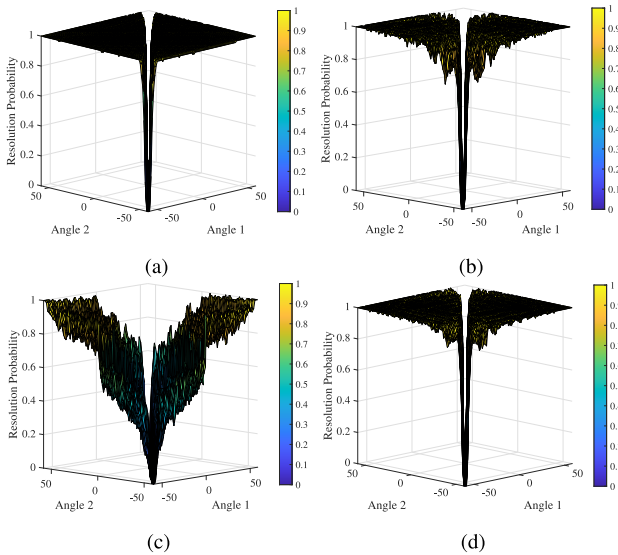


Fig. 4. Resolution probability for DOA estimation versus arbitrary angle variation when using (a) the proposed method, (b) Baseline 1, (c) Baseline 2, and (d) Baseline 3 with $M = 24$ and SNR = 0 dB.

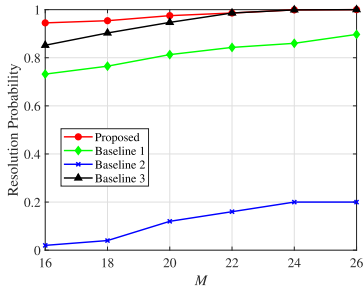


Fig. 5. Resolution probability of DOA estimation using the proposed method and baselines versus M with SNR = 0 dB.

of M . The results show that both the proposed method and the Baseline 3 significantly outperform the random sensing matrix. Notably, when the number of measurements is below 22, the proposed method achieves a higher resolution probability than all other methods, demonstrating superior estimation performance with limited measurements.

V. CONCLUSION

In this letter, we proposed a novel reconfigurable coding design method for PMS-based DOA estimation. Specifically, we formulated the coding design as a mutual coherence minimization problem of the sensing matrix, and further reformulated it as a Frobenius norm minimization problem. To solve this problem, we developed an AO framework that combines semidefinite programming and Riemannian MO to obtain the reconfigurable coding matrix. Simulation results demonstrated the superior DOA estimation and resolution performance of the proposed method, as well as its ability to reduce the number of required measurements compared to existing approaches. Future work includes extending the method to dynamic targets and validating its performance under practical hardware conditions.

REFERENCES

- [1] X. Luo, Q. Lin, R. Zhang, H.-H. Chen, X. Wang, and M. Huang, “ISAC—A survey on its layered architecture, technologies, standardizations, prototypes and testbeds,” *IEEE Commun. Surveys Tuts.*, early access, Apr. 29, 2025, doi: [10.1109/COMST.2025.3565534](https://doi.org/10.1109/COMST.2025.3565534).
- [2] R. Zhang, B. Shim, and W. Wu, “Direction-of-arrival estimation for large antenna arrays with hybrid analog and digital architectures,” *IEEE Trans. Signal Process.*, vol. 70, pp. 72–88, 2022.
- [3] M. Hua, Q. Wu, W. Chen, Z. Fei, H. C. So, and C. Yuen, “Intelligent reflecting surface-assisted Localization: Performance analysis and algorithm design,” *IEEE Wireless Commun. Lett.*, vol. 13, no. 1, pp. 84–88, Jan. 2024.
- [4] X. Gao, L. Dai, and A. M. Sayeed, “Low RF-complexity technologies to enable millimeter-wave MIMO with large antenna array for 5G wireless communication,” *IEEE Commun. Mag.*, vol. 56, no. 4, pp. 211–217, Apr. 2018.
- [5] R. Zhang, W. Wu, X. Chen, Z. Gao, and Y. Cai, “Terahertz integrated sensing and communication-empowered UAVs in 6G: A transceiver design perspective,” *IEEE Veh. Technol. Mag.*, early access, Feb. 17, 2025, doi: [10.1109/MVT.2025.3531088](https://doi.org/10.1109/MVT.2025.3531088).
- [6] L. Yao, R. Zhang, C. Hu, and W. Wu, “Off-grid DOA estimation for metasurface antenna systems using sparse Bayesian learning,” *Int. J. Electron. Commun.*, vol. 190, Feb. 2025, Art. no. 155615.
- [7] M. Hua, G. Chen, K. Meng, S. Ma, C. Yuen, and H. Cheung So, “3D multi-target localization via intelligent reflecting surface: Protocol and analysis,” *IEEE Trans. Wireless Commun.*, vol. 23, no. 11, pp. 16527–16543, Nov. 2024.
- [8] R. Zhang et al., “Tensor-based channel estimation for extremely large-scale MIMO-OFDM with dynamic metasurface antennas,” *IEEE Trans. Wireless Commun.*, vol. 24, no. 7, pp. 6052–6068, Jul. 2025.
- [9] Q. Wu et al., “Intelligent reflecting surfaces for wireless networks: Deployment architectures, key solutions, and field trials,” *IEEE Wireless Commun.*, early access, May 19, 2025, doi: [10.1109/MWC.001.250002](https://doi.org/10.1109/MWC.001.250002).
- [10] J. An et al., “Two-dimensional direction-of-arrival estimation using stacked intelligent metasurfaces,” *IEEE J. Sel. Areas Commun.*, vol. 42, no. 10, pp. 2786–2802, Oct. 2024.
- [11] T. J. Cui et al., “Coding metamaterials, digital metamaterials and programmable metamaterials,” *Light, Sci. Appl.*, vol. 3, no. 10, p. e218, 2014.
- [12] D. Xia et al., “Accurate 2-D DOA estimation based on active metasurface with nonuniformly periodic time modulation,” *IEEE Trans. Microw. Theory Technol.*, vol. 71, no. 8, pp. 3424–3435, Aug. 2023.
- [13] M. Lin et al., “Single sensor to estimate DOA with programmable metasurface,” *IEEE Internet Things J.*, vol. 8, no. 12, pp. 10187–10197, Mar. 2021.
- [14] J. Wang et al., “High-precision direction-of-arrival estimations using digital programmable metasurface,” *Adv. Intell. Syst.*, vol. 4, no. 4, 2022, Art. no. 2100164.
- [15] P. Chen, Z. Chen, B. Zheng, and X. Wang, “Efficient DOA estimation method for reconfigurable intelligent surfaces aided UAV swarm,” *IEEE Trans. Signal Process.*, vol. 70, pp. 743–755, 2022.
- [16] S. Lin, J. An, L. Gan, and M. Debbah, “UAV-mounted SIM: A hybrid optical-electronic neural network for DoA estimation,” in *Proc. IEEE ICASSP*, 2025, pp. 1–5.
- [17] B. Li, S. Zhang, L. Zhang, X. Shang, C. Han, and Y. Zhang, “Robust sensing matrix design for the orthogonal matching pursuit algorithm in compressive sensing,” *Signal Process.*, vol. 227, Feb. 2025, Art. no. 109684.
- [18] J. Lee, G.-T. Gil, and Y. H. Lee, “Channel estimation via orthogonal matching pursuit for hybrid MIMO systems in millimeter wave communications,” *IEEE Trans. Commun.*, vol. 64, no. 6, pp. 2370–2386, Jun. 2016.
- [19] X. Yu, J.-C. Shen, J. Zhang, and K. B. Letaief, “Alternating minimization algorithms for hybrid precoding in millimeter wave MIMO systems,” *IEEE J. Sel. Topics Signal Process.*, vol. 10, no. 3, pp. 485–500, Apr. 2016.
- [20] X. Ge, W. Shen, C. Xing, L. Zhao, and J. An, “Training beam design for channel estimation in hybrid mmWave MIMO systems,” *IEEE Trans. Wireless Commun.*, vol. 21, no. 9, pp. 7121–7134, Sep. 2022.
- [21] J.-C. Chen, “Low-PAPR precoding design for massive multiuser MIMO systems via Riemannian manifold optimization,” *IEEE Commun. Lett.*, vol. 21, no. 4, pp. 945–948, Apr. 2017.
- [22] Y. Ma and Y. Fu, *Manifold Learning Theory and Applications*. Boca Raton, FL, USA: CRC Press, 2012.
- [23] Y. Geng, T. Hiang Cheng, K. Zhong, and K. Chan Teh, “Unified manifold optimization for double-IRS-aided MIMO communication,” *IEEE Commun. Lett.*, vol. 28, no. 7, pp. 1713–1717, Jul. 2024.